J Sol-Gel Sci Technol (2015) 74:352–356
DOI 10.1007/s10971-014-3517-z

ORIGINAL PAPER

Sol–gel synthesis and investigation of structural, electrical and magnetic properties of Pb doped $La_{0.1}Bi_{0.9}FeO_3$ multiferroics

Imran Ghafoor · Saadat Anwar Siddiqi · Shahid Atiq · Saira Riaz · Shahzad Naseem

Received: 10 January 2014 / Accepted: 16 September 2014 / Published online: 30 September 2014

Abstract A sol–gel based auto-combustion technique has been employed to synthesize polycrystalline $La_{0.1}Bi_{0.9-x}Pb_xFeO_3$ (x = 0.0, 0.05, 0.10, 0.20, 0.30) ceramics. The samples have been characterized by X-ray diffraction, scanning electron microscopy, an LCR-meter and a vibrating sample magnetometer for their structural and morphological features, as well as electrical and magnetic properties, respectively. The structural analysis revealed that when Pb was doped at Bi-sites in $La_{0.1}Bi_{0.90}FeO_3$, the host retained the rhombohedrally distorted perovskite structure, attributed to the non centro-symmetric space group R3c. The surface morphological studies revealed that the grain size was increased and formed agglomerates at high concentrations of Pb contents. The dielectric parameters displayed conventional ferrite behavior depicting high values at low frequencies and decreasing with rise in frequencies, leading to constant values at still higher frequencies. The magnetic properties were changed non-monotonically with increasing Pb concentration. This non-monotonical behavior with increasing Pb could be attributed to the canting of the antiferromagnetic spins in $BiFeO_3$ based multiferroics.

Keywords Multiferroics · Magnetoelectric coupling · Magnetic properties · Electrical properties

I. Ghafoor · S. Atiq (✉) · S. Riaz · S. Naseem
Centre of Excellence in Solid State Physics, University of the Punjab, Quaid-e-Azam campus, Lahore 54590, Pakistan
e-mail: satiq.cssp@pu.edu.pk; shahidatiqpasrur@yahoo.com

S. A. Siddiqi
Interdisciplinary Research Centre in Biomedical Materials (IRCBM), COMSATS Institute of Information Technology, Defence Road, Off Raiwind Road, Lahore, Pakistan

1 Introduction

Multiferroics are the multi-functional materials that exhibit more than one ferroic properties (ferro-electricity, ferro-magnetism and ferro-elasticity) in the same phase, simultaneously [1]. Currently, the research community uses the term 'multiferroics' only for the materials that exhibit both ferro-electricity and magnetism (not necessarily ferro-magnetism) [2–4] owing to their potential device applications and fascinating fundamental physics. Low temperature magnetic ordering and weak coupling between magnetism and polarization are, hitherto, a hindrance in the application of these novel materials in devices [5]. $BiFeO_3$ (BFO) is the only material that has ferroelectricity (1103 K) and antiferro-magnetism (643 K) above room temperature (RT) and due to this reason BFO is the most studied material [6]. However, low resistivity, weak ferromagnetism in bulk BFO and its long range cycloildal spin structure have been obstacles in further device applications [5, 7]. The valance fluctuations on Fe ions and the existence of second phases are the causes of low resistivity and they can be suppressed by optimizing the fabrication process [7]. The suppression of spin configuration is a necessary condition for spontaneous magnetization and linear magnetic effect in BFO [8] and can occur through Dzyaloshinskii-Moriya interactions [9]. This suppression can be achieved by applying large magnetic or electric fields [10], producing epitaxial strains in thin films [11] and by doping the BFO with suitable ions of transition elements.

B-site doping in BFO, i.e., the substitution of Fe^{3+} by other transition metal ions has revealed the spontaneous magnetization but this doping decreases the magnetic transition temperature drastically. Further, it requires high pressure synthesis techniques to prepare the samples [12]. An enhancement of net magnetization has also been reported

by A-site substitution with the rare earth magnetic ions like Tb^{3+} [13], Nd^{3+} [14], Sm^{3+} [15] and Pr^{3+} [16]. The research on A-site doping with diamagnetic ions, for instance, in $Bi_{1-x}A_xFeO_3$ (A = La, Ba, Pb, Sr, Ca) has been proved to be important for the investigation of the influence of crystal chemistry on weak ferromagnetic moment values and thus can contribute to the development of relationship between the crystal structure, magnetic properties and magnetoelectric coupling in BFO based compounds [17–24].

In addition, Khomchenko et al. [19] doped the diamagnetic (Ca, Sr, Pb, Ba) ions and found that the value of the net magnetization strongly depended on the kind of diamagnetic element. The magnetization increased with the increase in ionic radii of the dopant element and the maximum value was achieved for the Ba^{3+} (1.2 emu/g) which had the biggest ionic radii among the other elements. Some groups [21–23] have concentrated on the Pb doping in BFO because of the fact that ionic radii of Pb^{3+} (133 pm) is larger than Bi^{3+} (117 pm) and can give enhanced magnetization. For example, Khomchenka et al. [5] synthesized $Bi_{0.80}Pb_{0.2}FeO_3$ sample by a rapid two stage solid state reaction method and carried out its magnetic, dielectric and ferroelectric measurements along with Mossbauer spectroscopy. They got a net magnetization at RT. Mazumder et al. [21] studied the dielectric and ferroelectric properties of lightly Pb doped BFO and were able to get improved dielectric properties. Zhang et al. [22] used the solid state solution reaction route to get Pb doped $Bi_{1-x}Pb_XFeO_3$ (x = 0.0, 0.1, 0.2, 0.3) and observed the ferroelectricity and magnetism at RT. Recently Ge et al. [23] have worked on Pb-La co-doping in BFO in the form of $Bi_{1-x}La_{0.2}Pb_xFeO_3$ (x = 0–0.2) ceramics. Their studies show that the magnetic properties vary non-monotonically whereas ferroelectric properties change monotonically with increasing x. In the present study, we have used a novel sol–gel based auto-ignition technique to prepare $La_{0.1}Bi_{0.9-x}Pb_xFeO_3$ (x = 0.0, 0.05, 0.1, 0.2, 0.3) ceramic samples, in order to investigate systematically the effect of Pb doping at Bi-site in $La_{0.1}Bi_{0.9}FeO_3$ on the structural, electrical and magnetic properties.

2 Experimental details

Polycrystalline samples of pure and Pb-doped bismuth ferrite having general formula as $La_{0.1}Bi_{0.9-x}Pb_xFeO_3$ (x = 0.0, 0.05, 0.10, 0.20 and 0.30) were prepared by using sol–gel auto-combustion method. The analytical grade starting reagents such as $Bi(NO_3)_3{\cdot}5H_2O$, $Fe(NO_3)_3{\cdot}9H_2O$, $Pb(NO_3)_3$, $La(NO_3)_3$ and glycine, used as a fuel, were mixed in 100 mL of water in stoichiometric amounts adjusting the metal nitrate (MN) to fuel ratio of 1:1.5. A few drops of concentrated nitric acid were added to dissolve the bismuth nitrate. Lanthanum nitrate was added to stabilize the crystalline phase of bismuth ferrite. The solution was stirred and heated at 90 °C for 2 h to get a gel. After gel formation, the temperature of the hotplate was raised up to 300 °C for complete combustion of the gel. After powder formation, the samples were calcined at 600 °C in a muffle furnace for 4 h. The samples were palletized having diameter of 16 mm using an Apex hydraulic press by applying a pressure 4.5 ton and then the samples were again sintered at 600 °C for 1 h.

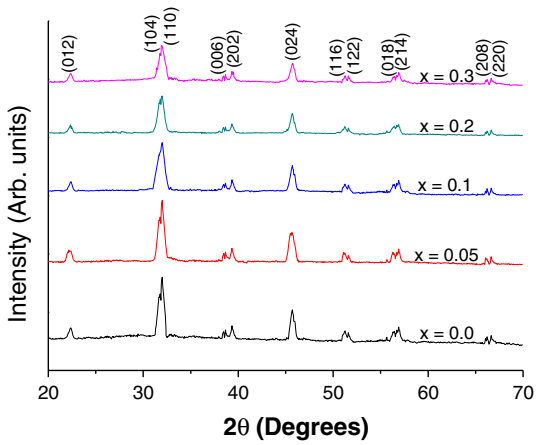

Fig. 1 X-ray diffraction patterns of $La_{0.1}Bi_{0.9-x}Pb_xFeO_3$ (x = 0.0, 0.05, 0.10, 0.20 and 0.30) samples

A Rigaku Ultimate IV, USA X-ray diffractometer (XRD) with CuK_α radiations (1.5418 Å) was used to record the diffraction patterns of powder samples to verify the formation of desired phase of the material. Surface morphology of the samples in the pallet form was investigated by a Jeol 3400S scanning electron microscope (SEM). Frequency (100 Hz–1 MHz) and temperature (40–200 °C) dependent dielectric characteristics of the ferroic samples were analyzed by a Quad-Tech 1920 LCR meter. A Lakeshore 7404 vibrating sample magnetometer (VSM) was utilized to determine the magnetic behavior of the samples.

3 Results and discussion

Figure 1 shows the diffraction patterns of $La_{0.1}Bi_{0.9-x}Pb_xFeO_3$ (x = 0.0, 0.05, 0.10, 0.20 and 0.30) samples. All the peaks present in the patterns were indexed according to the JCPD card no. 01-071-2494, characteristic of pure BFO, having a rhombohedral symmetry with the space group R3c. No impurity peaks relating to any secondary phase were detected in the patterns. It is inferred that a MN to fuel ratio of 1:1.5 and a heat treatment at 600 °C for 4 h, are quite optimum conditions to prepare these samples.

In R3c space group, the cations are displaced from their centrosymmetric positions along the threefold symmetric

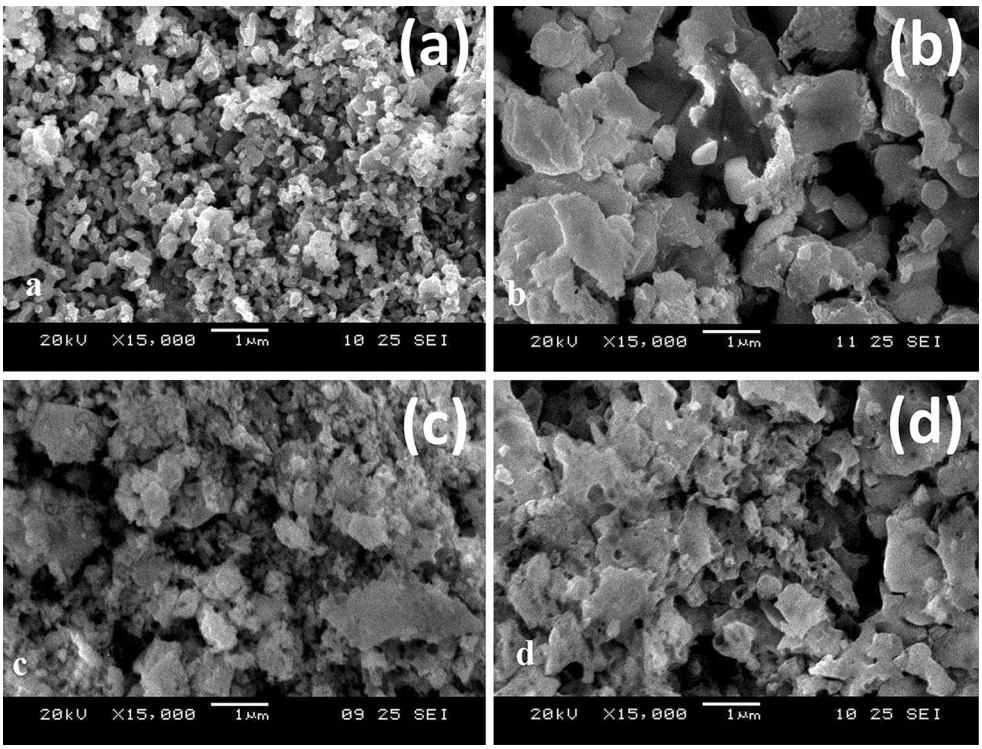

Fig. 2 SEM micrographs of $La_{0.1}Bi_{0.9-x}Pb_xFeO_3$ with x = (**a**) 0.0, (**b**) 0.10, (**c**) 0.20 and (**d**) 0.30

hexagonal [001] axes and produce polarization. In case of BFO, polarization is obtained by the antiphase tilt of adjacent FeO_6 octahedra, and by the displacements of Fe^{3+} and Bi^{3+} cations along [111] directions from their centrosymmetric positions [18]. The diffraction patterns of the samples in the series show that the intensity of the diffraction peaks decrease a bit with the increase in Pb doping. Since the peak intensity is related to the amplitude of rotation of the octahedra [22], so the amplitude of tilt of rhombohedral distortion reduces and hence it is inferred that polarization reduces with increasing Pb doping.

It has been reported in a previous study that the substitution of an ion with larger radii to that of a relatively smaller radii results in the peak shift towards larger 2θ values [16]. This in turn results in the contraction of the lattice parameters and the unit cell volume of all the samples. To confirm, lattice parameters and unit cell volume were also evaluated using the software "CELL". A slight decrease in the cell parameters and hence in the unit cell volume was observed as the amount of dopant Pb was increased in the series that could be attributed to the fact that substitution of heterovalent Pb^{2+} on Bi^{3+} required the appearance of oxygen vacancies or/and Fe^{4+} ions in the lattice due to which unit cell volume might reduce [5].

Surface morphology of the samples in pellet form was analyzed by SEM. The micrographs of the samples obtained at a resolution of 15× k have been shown in Fig. 2. The micrograph of the sample without Pb doping (Fig. 2a) reveals uniform sized grains distributed homogenously over the surface. The grain boundaries are obvious and can be marked precisely. The estimated grain sizes were in the range of 150–200 nm. Three representative micrographs of Pb-doped samples have also been shown in Fig. 2b–d. It has been seen that the grain sizes are increased drastically in these samples and porosity has also been increased. Some of the large sized grains could also be termed as agglomerates of the small sized grains. Anyhow, sharp and well-defined boundaries can also be marked in Pb-doped samples.

The frequency dependent dielectric measurements were taken in the frequency range of 100 Hz–1 MHz at RT, as can be seen in Fig. 3. The plots reveal that the dielectric constant of all the samples have large values at low frequencies (100 Hz) and decrease abruptly as the frequency increases. After a specific frequency value, the dielectric factors do not change and remain almost constant up to about 1 MHz. This dielectric anomaly with frequency can be considered to be due to the combine response of dielectric relaxation which involves the oriental polarization and the conduction of charge carriers [25]. These processes could well be explained on the basis of Maxwell–Wagner model [26]. At low frequencies, the rotator

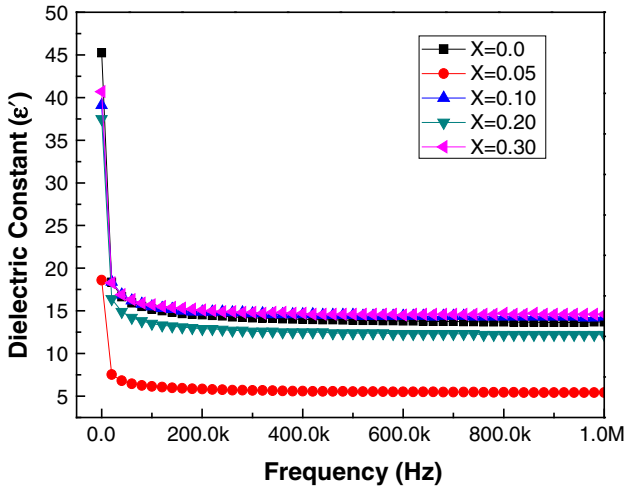

Fig. 3 Dielectric constant as a function of applied frequency for the $La_{0.1}Bi_{0.9-x}Pb_xFeO_3$ (x = 0.0, 0.05, 0.10, 0.20 and 0.30) samples

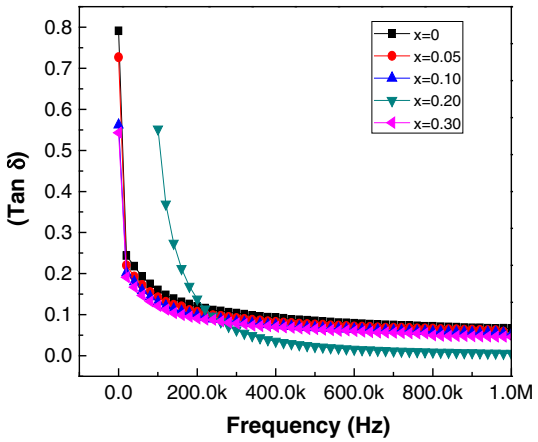

Fig. 4 Dielectric tangent loss as a function of applied frequency for the $La_{0.1}Bi_{0.9-x}Pb_xFeO_3$ (x = 0.0, 0.05, 0.10, 0.20 and 0.30) samples

motion of all the polar molecules of the dielectric material is rapid enough to follow the applied field and hence gives large dielectric constant values. On the other hand at higher frequencies, the motion lags behind the alternating fields and give low dielectric constant values. The dielectric tangent loss also follows the same trend as dielectric constant as shown in Fig. 4. Similar trend of dielectric properties has also been reported in Mn [27], Sr [28], Sm [15], Pr [16], and Dy [29] doped BFO materials. The temperature dependent dielectric parameters were studied in the temperature range of 40–200 °C. Figure 5 shows the trend of tangent loss with the increase of temperature for the doped and un-doped samples while the inset shows the behavior of dielectric loss in the same temperature range. A slight increase in these dielectric parameters was evident

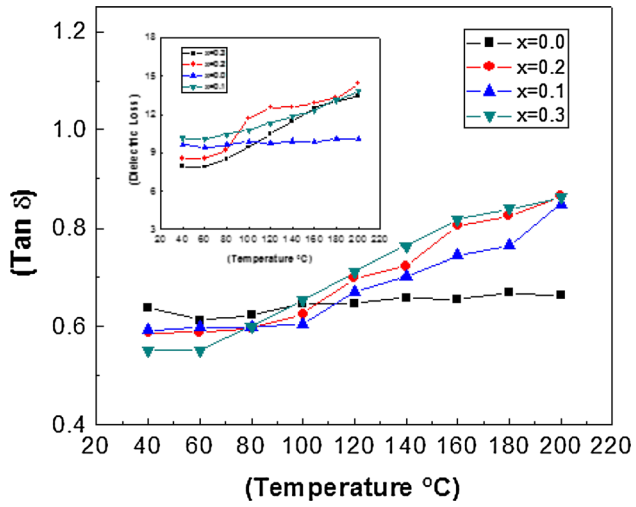

Fig. 5 Dielectric tangent loss as a function of temperature for the $La_{0.1}Bi_{0.9-x}Pb_xFeO_3$ (x = 0.0, 0.05, 0.10, 0.20 and 0.30) samples. The *inset* shows the trend of dielectric loss for the same temperature range

with the rise of temperature. This rise can be attributed to the thermally induced enhancement of hopping conduction mechanism [21, 30].

Figure 6 shows the magnetic hysteresis (M-H) loops of un-doped and Pb-doped samples obtained at RT by applied magnetic field of 12 kOe. As obvious from the M-H loops, the value of saturation magnetization (M_s), remanence (M_r) and coercivity (H_c) increase as the Pb is doped. At the same time, an anomaly occurs for x = 0.1, where the M_s, M_r and H_c values are seemed to decrease. However, with further doping of Pb (i.e. for x = 0.2, 0.3) these magnetic parameters were seemed to increase again. This non-monotonic reliance of magnetization on the amount of dopant shows the probability of tuning the magnetic ordering in BFO by composition adjustment during co-doping. Generally, the introduction of net magnetization in $La_{0.1}Bi_{1-x}Pb_xFeO_3$ (x = 0.0, 0.05, 0.10, 0.20 and 0.30) can be attributed to the following mechanisms. First, the doping of diamagnetic ion (Pb^{2+}) seems to create oxygen vacancies and/or Fe^{4+} ions in the BFO ceramics. As the superexchange interactions for both Fe^{3+}–O–Fe^{3+} and Fe^{3+}–O–Fe^{4+} are antiferromagnetic, so they give zero net magnetization [18, 19]. Ederer et al. [24] have proposed that oxygen vacancies are not able to affect the canting of the magnetic moments and hence could not enhance net magnetization. Secondly, the A-site doping can change the anisotropy constant and becomes a cause to change the spin structure of BFO from spatially modulated spin structure to a homogeneous canted one [31]. Therefore, it is likely that the structural distortion has canted the antiferromagnetic spins and induced net magnetization in our samples. The

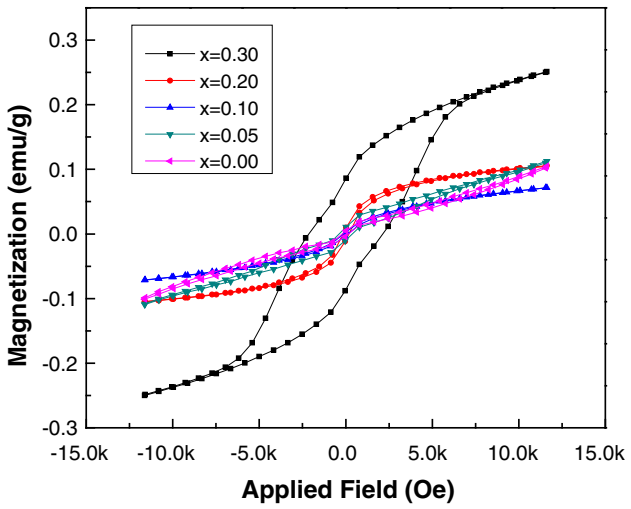

Fig. 6 A comparison of M-H loops of $La_{0.1}Bi_{0.9-x}Pb_xFeO_3$ (x = 0.0, 0.05, 0.1, 0.2 and 0.3) samples

La doping changes the structure of BFO from rhombohedral to pseudotetragonal [23] whereas Pb doping changes its structure to pseudocubic [22, 23]. Further these dopings suppress the spin structure in opposite to each other and when doping of La and Pb are equal, they may cancel the effect of each other, resulting in reduction in the latent magnetization. This might be the cause of low magnetization and remanance at x = 0.1. At x = 0.3, the structural transformation from rohmbohedral to pseudocubic is almost complete and destroys the spatial spin structure [22] resulting in large latent magnetization as compared to other samples.

4 Conclusion

The effect of Pb (A-site diamagnetic ion) doping on the crystal structure, surface morphology, dielectric and magnetic properties of $La_{0.1}Bi_{0.9-x}Pb_xFeO_3$ (x = 0.0, 0.05, 0.10, 0.20 and 0.30) samples, prepared by sol–gel auto-ignition technique, have been investigated systematically. The XRD analysis reveals that all the samples have single phase perovskite structure which can be described by space group R3c. Lattice constant and unit cell volume decrease with the Pb doping. The surface morphology of material changes with the increase in concentration of Pb in the host materials and an increase in grain size and porosity of the samples is evident. The frequency dependent dielectric anomaly is due to the dielectric relaxation whereas the increase in dielectric factors with rising temperature is related to thermally induced enhancement of the hopping conduction. The Pb doping at Bi-site in $La_{0.1}Bi_{0.9}FeO_3$ has been understood to suppress the spiral spin structure to a canted spin structure by enhancing its net magnetization but this suppression is non-monotonical with respect to increasing x.

References

1. Kreisel J, Kenzelmann M (2009) Europhys News 40:17
2. Khomskii D (2009) Phys Today 20:1
3. Cheong SW, Mostovoy M (2007) Nat Mater 6:13
4. Khomskii DI (2006) J Magn Magn Mater 306:1
5. Khomchenko VA, Kiselev DA, Vieira JM, Rubinger RM, Sobolev NA, Kopcewicz M, Shvartsman VV, Borisov P, Kleemann W, Kholkin AL (2008) J Phys Condens Mater 20:155207
6. Spaldin NA, Cheong SW, Ramesh R (2010) Phys Today 63:38
7. Ramesh R, Spaldin NA (2007) Nat Mater 6:21
8. Kadomtseva AM, Zvezdin AK, Popov YF, Pyatakov AP, Vorob'ev GP (2004) JETP Lett 79:0571
9. Sergienko IA, Dagotto E (2006) Phys Rev B 73:094434
10. Ruette B, Zvyagin S, Pyatakov AP, Bush A, Li JF, Belotelov VI, Zvezdin AK, Viehland D (2004) Phys Rev B 69:064114
11. Bai F, Wang J, Wutting M, Li JF, Wang N, Pyatakov AP, Zvezdin AK, Cross LE, Viehl D (2005) Appl Phys Lett 86:032511
12. Azuma M, Takata K, Saito T, Ishiwata S, Shimakawa Y, Takano M (2005) J Am Chem Soc 127:8889
13. Palkar VR, Kundaliya DC, Malik SK, Bhattacharya S (2004) Phys Rev B 69:212102
14. Yuan GL, Or SW, Liu JM, Liu ZG (2006) Appl Phys Lett 89:052905
15. Yuan GL, Or SW (2006) J Appl Phys 100:024109
16. Uniyal P, Yadav KL (2009) J Phys Condens Matter 21:405901
17. Khomchenko VA, Kiselev DA, Kopcewicz M, Maglione M, Shvartsman VV, Borisov P, Kleemann W, Lopes AML, Pogorelov YG, Araujo JP, Rubinger RM, Sobolev NA, Vieira JM, Kholkin AL (2009) J Magn Magn Mater 321:1692
18. Khomchenko VA, Kiselev DA, Vieira JM, Khalkin AL (2007) Phys Rev 90:242901
19. Khomchenko VA, Kiselev DA, Selezneva KE, Vieira JM, Aravjo JP, Kholkin AL (2008) Mater Lett 62:1927
20. Troyanchunk IO, Bushinsky MV, Karpinsky DV, Sirenkc V, Silkolenko V, Elimor V (2010) Europhys Rev 73:375
21. Mazumder R, Sen A (2009) J Alloys Compd 475:577
22. Zhang X, Sui Y, Wang X, Tang J, Su W (2009) J Phys Condens Matter 105:07D918
23. Ge JJ, Xue XB, Cheng GF, Yang M, You B, Zhang W, Wu XS, Hu A, Du J, Zhang SJ, Zhou SM, Wang Z, Yang B, Sun L (2011) J Phys Condens Matter 324:200
24. Ederer C, Spaldin NA (2005) Phys Rev B 71:224103
25. Khomchenko VA, Kiselev DA, Vieira JM, Jian L, Kholkin AL, Lopes ALM, Pogorelov YG, Araujo JP, Maglione M (2008) J Appl Phys 103:024105
26. Wang N, Cheng J, Pyatakov A, Zvezdin AK, Li JF, Cross LE, Viehland D (2005) Phys Rev B 72:104434
27. Reetu, Agarwal A, Sanghi S, Ashima (2011) J Appl Phys 110:073909
28. Wagner KW (1913) Ann Phys 40:817
29. Sahu JR, Rao CNR (2007) Solid State Sci 9:950
30. Bhushan B, Basumallick A, Vasanthacharya NY, Kumar S, Das D (2010) Solid State Sci 12:1063
31. Li Y, Yu J, Li J, Zheng C, Wu Y, Zhao Y, Wang M, Wang Y (2011) J Mater Sci Mater Electron 22:323